Micro-Raman study of orbiton-phonon coupling in YbVO3

Roberge, B.; Jandl, S.; Nugroho, A. A.; Palstra, T. T. M.

Published in:
Journal of Raman Spectroscopy

DOI:
10.1002/jrs.3006

Publication date:
2012

Research Article

Journal of RAMAN SPECTROSCOPY

Received: 24 March 2011 Accepted: 4 May 2011 Published online in Wiley Online Library: 28 June 2011

(wileyonlinelibrary.com) DOI 10.1002/jrs.3006

Micro-Raman study of orbiton–phonon coupling in $YbVO_3$

B. Roberge,[a] S. Jandl,[a]* A. A. Nugroho[b] and T. T. M. Palstra[c]

First-order and multiphonon Raman active excitations are studied in $YbVO_3$ as a function of temperature in the orthorhombic and monoclinic phases. Below $T \simeq 170$ K, a G-type orbital ordering with a concomitant monoclinic transition occurs. They enhance the phonon polarizabilities, allowing the resolution of room-temperature bands, and activate new excitations around 700 cm^{-1}. Below $T \sim 65$ K, the 700 cm^{-1} excitations disappear, indicating a C-type orbital ordering and a return to the orthorhombic structure. The observed phonon combinations around 1400 cm^{-1} with a dominant Jahn-Teller vibration at ~690 cm^{-1} reflect a possible orbiton-phonon coupling. Copyright © 2011 John Wiley & Sons, Ltd.

Keywords: micro-Raman; YbVO3; phonon; orbiton; phase transitions

Introduction

Owing to their strong electron correlation, transition-metal oxides with perovskite-related structures display a variety of interesting properties such as Mott transition, high-T_c superconductivity and colossal magnetoresistance. They are prototypes for the interplay among the charge, orbital, spin and lattice excitations. Usually for cations with orbital degeneracy such as Mn^{3+}, Ni^{3+}, Ti^{3+} and V^{3+}, long-range orderings of the occupied *d* orbitals accompanied by a Jahn–Teller distortion are expected at low temperatures.[1]

Orbitons or low-energy multipolar charge excitations are associated with the modulations of the electronic cloud shapes in transition-metal oxides ordered states.[2] They represent a dynamical response that propagates between the transition-metal ion orbitals and are considered as potential candidate for ultrafast switching. The Raman scattering study of $LaMnO_3$ that claimed orbiton detection[3] has been thoroughly contested.[4–7] In the case of YVO_3, while Sugai and Hirota[8] identified the 679 cm^{-1} Raman active excitation as orbiton and the 489 cm^{-1} excitation as phonon, Miyasaka *et al*.[9] reversed their identifications as phonon and orbiton, respectively. In a preliminary study, Jandl *et al*.[10] have shown that Raman excitations observed in $YbVO_3$ and YVO_3 were of phonon origin.

In their study of the $RMnO_3$ (R = rare earth) manganites, and based on polarization properties, lattice-dynamics calculation and oxygen isotope substitution, Iliev *et al*.[7] have shown that all the excitations attributed to orbitons by Saitoh *et al*.[3] are rather of phonon nature. Also, the Raman study of $RMnO_3$ multiphonons by Laverdière *et al*.[5] indicated a possible coupling of orbiton to the lattice with an intermediate electron–phonon strength.[11]

At room temperature, the RVO_3 crystallographic structure is orthorhombic with typical *Pnma* space group parameters $a \simeq c \simeq \sqrt{2}a$ and $b \simeq 2a$, where a is the lattice parameter of the ideal cubic perovskite. The V^{3+} ions have two t_{2g} d electrons with coupled parallel spins ($S = 1$) according to Hund's rule. One electron occupies the *ac* orbital whose energy is lowered because of the orthorhombic distortion which reduces the crystal-field symmetry. The other electron occupies either the *ab* or the *bc* orbital.[12] The two electron spins align ferromagnetically along the *b*-axis and antiferromagnetically in the *ac* plane (C-type spin), while the d_{ab} and d_{bc} orbitals, respectively, alternate (G-type orbit).[13,14] The C-type spin and G-type orbit transition temperatures depend on the ionic radius of the R ion. The Jahn–Teller distortion increases for the small R ionic radius, whereas the V–O–V bond angle deviates from 180° and the transfer interaction as well as the spin and orbital interactions decrease between the V^{3+} nearest neighbors. In the case of large Jahn–Teller distortions, a second transition characterized by a magnetization reversal occurs at a lower temperature (e.g. in YVO_3). The spins align this time antiferromagnetically along the *b*-axis (G-type spin) with identical orbits (either d_{ab} or d_{bc}) along the *b*-axis alternating in the *ac* plane (C-type orbit). According to Ulrich *et al*.,[15] the spin exchange interaction parameters J_{ac} and J_b are of the order of 5.7 ± 3 meV in the G-type spin-ordered state in YVO_3. This translates in two magnon excitations of the order of 60 meV.[16]

Polycrystalline samples of $YbVO_3$ have been studied by neutron powder diffraction, specific heat and magnetization measurements.[17] At room temperature, the crystal structure is orthorhombic ($a = 5.5662(2)$ Å, $b = 7.5446(2)$ Å, $c = 5.2320(1)$ Å). An orbital ordering effect is observed around 170 K, coinciding with an anomaly in the specific heat, concomitant with a change in the thermal variations of the *a* and *b* parameters and the V–O distances. Below $T_N = 104$ K, $YbVO_3$ becomes magnetically ordered with the magnetic moments antiferromagnetically coupled in the *ac* plane.[17]

In this study of the first-order and multiphonon Raman active excitations in $YbVO_3$, we report their evolutions as a function of

* *Correspondence to: S. Jandl, Department of Physics, University of Sherbrooke, Sherbrooke, Quebec, J1K2R1, Canada. E-mail: serge.jandl@usherbrooke.ca*

a *Department of Physics, University of Sherbrooke, Sherbrooke, Quebec, J1K2R1, Canada*

b *Department of physics, Faculty of Mathematics and Natural Sciences, Institut Teknologi Bandung, 40132 Bandung, Indonesia*

c *Department of Physics, Zernike Institute for Advanced Materials, Rijksuniversiteit Groningen, Groningen, The Netherlands*

temperature and correlate them with the expected orbital and magnetic orders.

Experimental

The Raman spectra at 0.5 cm^{-1} resolution were measured in the backscattering configuration using a Labram-800 Raman microscope spectrometer equipped with a 50× (~0.35 mW μm^{-2}; 3 µm laser spot) magnification objective, and a nitrogen-cooled charge coupled device (CCD) detector. A He–Ne ($\lambda = 6328$ Å (1.96 eV)) laser, whose power was kept below 2 mW, and an appropriate notch filter were used with the samples mounted on the cold finger of a micro-Helium Janis cryostat. Polycrystalline samples of $YbVO_3$ were prepared by the chemical reduction of $YbVO_4$ powder obtained by high-temperature solid-state reaction of stoichiometric mixtures of pre-dried Yb_2O_3 and V_2O_5. $YbVO_4$ was then reduced by annealing the powder in a flow of pure H_2 at 1000 °C. A single-crystalline boule of ~6 mm in diameter and 60–70 mm in length was grown by the traveling solvent floating zone method. The crystallinity of the boule was checked by X-ray analysis and the composition by electron probe microanalysis.

Results and Discussion

The orthorhombic $YbVO_3$ primitive cell contains four molecular units resulting in $7A_g + 5B_{1g} + 7B_{2g} + 5B_{3g}$ Raman active modes.[9] The A_g modes are observed in the (*aa*), (*bb*) and (*cc*) configurations for the incident and scattered light polarizations as given in parenthesis, and the B_{1g}, B_{2g}, B_{3g} in the (*ab*), (*ac*), (*bc*) configurations, respectively. When the *Pnma* orthorhombic lattice symmetry is lowered to the monoclinic symmetry, the A_g and B_{2g} modes become A_g and the B_{1g} and B_{3g} modes become B_g modes, respectively.

At 300 K, the apical V–O distance along the b direction and the short V–O distance in the *ac* plane are almost identical (~1.985 Å). They diverge (~1.980 and 1.990 Å, respectively) below 170 K, resulting in orbital ordering and octahedral tilting.[17]

In the wide temperature range of 170–65 K, a cooperative Jahn–Teller distortion provokes a magnetostrictive crystallographic transition. It corresponds to an abrupt decrease of the *a*-lattice parameter magnitude, leading to a contraction of the unit cell volume. Simultaneously with the transition, a magnetic ordering that couples the magnetic moments antiferromagnetically in the *ac* plane and also along the *b*-axis occurs.[17]

In Fig. 1, Raman active excitations of $YbVO_3$ are shown as a function of temperature in the (*ac*) configuration allowing the B_{2g} symmetry phonons to be observed. At $T = 300$ K, two excitations are observed around 440 and 500 cm^{-1} and two broad bands around 325 and 680 cm^{-1}. The orbital ordering below 170 K enhances the phonon polarizabilities, allowing the resolution of the broad bands in four excitations: 325, 350, 680 and 700 cm^{-1}. The 350 cm^{-1} excitation corresponds to a leakage of the strongest A_g symmetry phonon and the 700 cm^{-1} to phonon density activated by orbital ordering as discussed below. Below $T_N = 104$ K and down to 65 K, the phonon bandwidths become narrower and the following B_{2g} phonons are better resolved: 327 cm^{-1} (out-of-phase *c*-rotation), 445 cm^{-1} (oxygen vibration along *c*-axis), 507 cm^{-1} (out-of-phase bending), 545 cm^{-1} (in-phase bending) and 681 cm^{-1} (in-phase oxygen stretching vibration) as described in analogy with $RMnO_3$ phonon

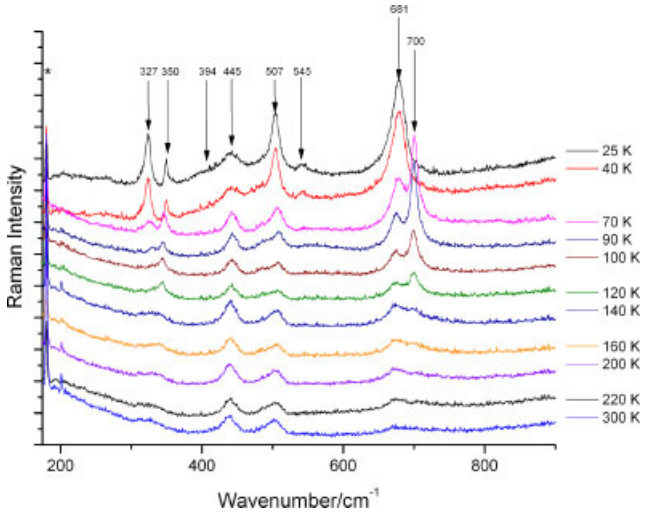

Figure 1. B_{2g} Raman active phonons in $YbVO_3$ as a function of temperature in the orthorhombic and monoclinic phases. '*' indicates plasma lines.

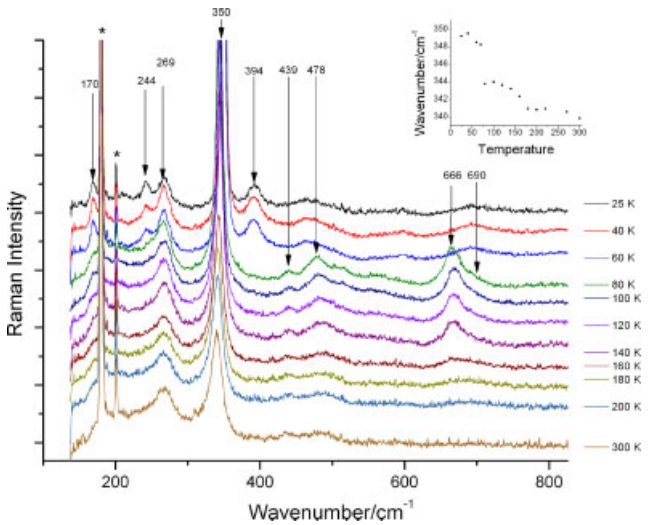

Figure 2. A_g Raman active phonons in $YbVO_3$ as a function of temperature in the orthorhombic and monoclinic phases. Inset: frequency of the 350 cm^{-1} phonon as a function of temperature. '*' indicates plasma lines.

and their corresponding lattice dynamical calculations.[18] Below $T \simeq 65$ K, following the complete alignment of the spins, a new two-magnon broad excitation around 475 cm^{-1} is observed, which is in agreement with the predictions of Ref. [16], while the 700 cm^{-1} excitation disappears.

In Fig. 2, Raman active excitations of $YbVO_3$ are shown as a function of temperature in the (*bb*) configuration allowing the A_g symmetry phonons to be observed. At $T = 180$ K, two excitations are observed at 267 cm^{-1} (VO_6 octahedra rotation) and 342 cm^{-1} (bending of the VO_6 octahedra) with broad bands around 450 and 700 cm^{-1}. Similar to the B_{2g} symmetry phonons, the orbital ordering below 170 K, with monoclinic lattice distortions, enhances the phonon polarizabilities and allow the observation of additional A_g modes at ~170 (Yb vibration along the *c*-axis), ~240, ~470 cm^{-1} (anti-stretching vibrations of oxygens in the *ac* plane) as well as some of the B_{2g} phonons (~440 and ~500 cm^{-1}) which are allowed now in the A_g symmetry. The broad band around 700 cm^{-1} is also resolved in two excitations around 666

and 690 cm^{-1}. Sensitivity of these modes to the phase transitions and crystal symmetry, with normal bandwidth broadenings at low temperatures, prompts us to rule out defects associated with oxygen non-stoichiometry and their corresponding unusual broad band Raman excitations as encountered in similar compounds.[19] At lower temperatures down to 65 K, the phonon bandwidths become narrower. Below $T \simeq 65$ K the A_g phonons (170, 244, 269, 350 and 394 cm^{-1}) are better resolved and the 439 and 500 cm^{-1} B_{2g} phonons as well as the 666 cm^{-1} excitation intensities drop, indicating a return to the orthorhombic symmetry and a change in the orbital ordering and resulting polarizabilities as observed in the evolution of the V–O distances between 104 and 65 K (2.020–1.985 Å for the long V–O distance in the *ac* plane and 2.000–2.025 Å for the short V–O distance in the *ac* plane[17]).

Various orderings below 170 and 65 K are observed in the strongest A_g mode (~350 cm^{-1}) wavenumber shifts as a function of temperature (Fig. 2, inset).

The first-order Raman active phonon temperature evolutions indicate a strong similarity with YVO_3 structural and orbital orderings as a function of temperature. Actually, the YVO_3 structure changes successively from orthorhombic *Pnma* space group at room temperature to monoclinic $P2_1/c$ space group at $T = 200$ K and back to *Pnma* space group at $T = 77$ K.[1,12] The increased tilting of the octahedra orders the orbitals in the G-type configuration below 200 K and in the C-type configuration below 77 K.[13,14]

Using a Hamiltonian that incorporates both superexchange and intermediate strength electron–phonon interaction that couples electrons to Jahn–Teller modes, Van den Brink[11] has shown that excitations of mixed orbiton–phonon character can arise. In the YVO_3 monoclinic phase and G-type configuration orbital, between 200 and 77 K, Sugai and Hirota[8] have associated the 675 cm^{-1} excitation to two-orbiton wave. Even if this identification cannot be definitely ruled out, we associate the 666 and 690 cm^{-1} (A_g symmetry excitations) and 700 cm^{-1} (B_{2g} symmetry excitation), which appear in the monoclinic phase, to phonon modes activated by orbital ordering as reported in YVO_3 for the 664 and 688 cm^{-1} excitations by Miyasaka *et al.*[9] and in $RMnO_3$ (R = Pr, Sm, Eu, Tb, Y) for the modes around 650 cm^{-1} by Laverdière *et al.*[5] It is noteworthy that in the case of $DyMnO_3$, the ~650 cm^{-1} excitation was also identified as of phonon origin based on polarization properties and in close comparison with the results of lattice-dynamics calculations.[7]

Figure 3(a) and (b) shows, in addition to the A_g and the B_{2g} phonons, Raman excitations up to 1600 cm^{-1} as a function of temperature. Multiphonons are observed as a broad band around 1380 cm^{-1} at 300 K in both symmetries. At lower temperatures, the band intensities are enhanced down to ~65 K, and then they decrease down to 20 K.

In addition to the excitations of mixed orbiton–phonon character, Van den Brink[11] has predicted a phonon pattern that repeats at the wavenumber interval (~650 cm^{-1}) of the on-site Jahn–Teller vibration (oxygen octahedron elongation along the *b*-axis and contraction in the *ac*-plane). Also, multiphonons are expected in the higher energy range with lower intensities than in the strong coupling regime. Similar to the study of $RMnO_3$ (R = Pr, Sm, Eu, Tb, Y), where multiphonons are separated by the Jahn–Teller mode wavenumber,[5] we associate the ~1380 cm^{-1} band with the phonon wavenumber combinations (666 + 690), (690 + 690) and (700 + 690) cm^{-1}. Also, the 690 cm^{-1} mode and the multiphonon intensities are correlated as a function of temperature and the 690 cm^{-1} mode predominates in the

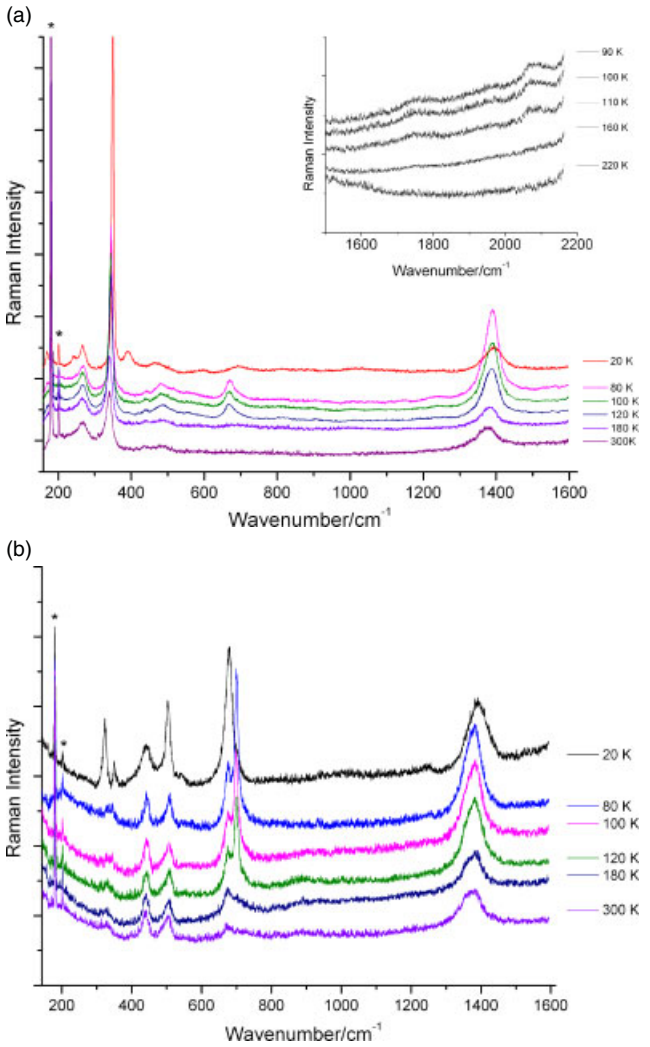

Figure 3. First- and second-order phonons in $YbVO_3$. (a) A_g symmetry, inset: third-order phonons; (b) B_{2g} symmetry. '*' indicates plasma lines.

phonon combinations as expected by the Jahn–Teller mode.[11] By comparing the intensities of the 666, 690 and 700 cm^{-1} excitations, the phonon combination intensities increase remarkably between first- and second-order processes and then decrease rapidly with their increasing order (inset, Fig. 3(a)) as previously observed in the manganites.[5,20] This indicates that the electron–phonon coupling constant g is of intermediate strength, as considered in Ref. [11], and not as strong as supposed in the localized limit with Franck–Condon processes[21] where intensities of the combination order n follow the power law g^n.

Conclusion

The A_g and B_{2g} Raman active phonons of $YbVO_3$ have been studied as a function of temperature retracing the various phase transitions observed by neutron powder diffraction, specific heat and magnetization measurements.[17] Hence, below 170 K a G-type orbital ordering is formed and new phonon density excitations around 700 cm^{-1} are activated in both A_g and B_{2g} symmetries associated with a transition from orthorhombic to monoclinic structure. Such excitations are particularly enhanced between

$T_N \sim 104$ K (C-type spin) and $T \sim 65$ K and vanish at lower temperatures. Similar to previous observations in YVO_3, a possible change to C-type orbital and G-type spin orders occurs.

High-energy phonon combinations are also observed, which reflect an intermediate strength electron–phonon coupling as described by Van den Brink within an orbiton–phonon coupling scheme Ref. [11].

Acknowledgements

The authors would like to thank M. Castonguay and M. Zakorzermy for experimental help and M. Poirier for valuable discussions. B. Roberge and S. Jandl acknowledge support from the National Science and Engineering Research Council of Canada and the Fonds Québécois de la Recherche sur la Nature et les Technologies.

References

[1] G. R. Blake, T. T. M. Palstra, Y. Ren, A. A. Nugroho, A. A. Menovsky, *Phys. Rev. Lett.* **2001**, *87*, 245501.
[2] S. Ishihara, J. Inoue, S. Maekawa, *Phys. Rev., B* **1997**, *55*, 8280.
[3] E. Saitoh, S. Okamoto, K. T. Takahashi, K. Tobe, K. Yamamoto, T. Kimura, S. Ishihara, S. Maekawa, Y. Tokura, *Nature* **2000**, *410*, 180.
[4] M. Grüninger, R. Rückamp, M. Windt, P. Reutler, C. Zobel, T. Lorenz, A. Freimuth, A. Revcolevschi, *Nature* **2002**, *418*, 39.
[5] J. Laverdière, S. Jandl, A. A. Mukhin, V. Yu Ivanov, *Eur. Phys. J. B* **2006**, *54*, 67.
[6] S. Jandl, J. Laverdière, A. A. Mukhin, V. Yu Ivanov, A. M. Balbashov, *Physica B* **2006**, *381*, 214.
[7] M. N. Iliev, V. G. Hadjiev, A. P. Litvinchuk, F. Yen, Y. Q. Wang, Y. Y. Sun, S. Jandl, J. Laverdière, V. N. Popov, M. M. Gospodinov, *Phys. Rev., B* **2007**, *75*, 064303.
[8] S. Sugai, K. Hirota, *Phys. Rev., B* **2006**, *73*, 020409.
[9] S. Miyasaka, J. Fujioka, M. Iwama, Y. Okimoto, Y. Tokura, *Phys. Rev., B* **2006**, *73*, 224436.
[10] S. Jandl, A. A. Nugroho, T. T. M. Palstra, *Proc. J. Phys.: Conf. ser.* **2010**, *200*, 032025.
[11] J. Van den Brink, *Phys. Rev. Lett* **2001**, *87*, 217202.
[12] G. R. Blake, T. T. M. Plastra, Y. Ren, A. A. Nugroho, A. A. Menovsky, *Phys. Rev. B* **2002**, *65*, 174112.
[13] Y. Ren, T. T. M. Palstra, D. I. Khomskii, E. Pellegrin, A. A. Nugroho, A. A. Menovsky, G. A. Sawatzky, *Nature* **1998**, *396*, 441.
[14] M. Noguchi, A. Nakazawa, S. Oka, T. Arima, Y. Wakabayashi, H. Nakao, Y. Murakami, *Phys. Rev. B* **2000**, *62*, R9271.
[15] C. Ulrich, G. Khaliullin, J. Sirker, M. Reehuis, M. Ohl, S. Miyasaka, Y. Tokura, B. Keimer, *Phys. Rev. Lett.* **2003**, *91*, 257202.
[16] M. J. Massey, N. H. Chen, J. W. Allen, R. Merlin, *Phys. Rev. B* **1990**, *42*, 8776.
[17] A. Munoz, J. A. Alonso, M. T. Casais, M. J. Martinaz-Lope, J. L. Martinez, M. T. Fernandez-Diaz, *J. Mater. Chem.* **2003**, *13*, 1234.
[18] M. N. Iliev, M. V. Abrashev, H. G. Lee, V. N. Popov, Y. Y. Sun, C. Thomsen, R. L. Meng, C. W. Chu, *Phys. Rev. B* **1998**, *57*, 2872.
[19] R. Laiho, K. G. Lisunov, E. Lähderanta, V. S. Stamov, V. S. Zakhvalinskii, Ph. Colomban, P. A. Petrenko, YP. Stepanov, *J. Phys. Condens. Matter* **2005**, *17*, 105.
[20] K. Y. Choi, P. Lemmens, G. Güntherodt, Y. G. Pashkevich, V. P. Gnezdilov, P. Reutler, L. Pinsard-Gaudart, B. Büchner, A. Revcolevschi, *Phys. Rev. B* **2005**, *72*, 024301.
[21] V. Perebeinos, P. B. Allen, *Phys. Rev. B* **1998**, *92*, 4828.